Department of Mechanical and Aerospace Engineering (MAE)Faculty and Researchers' Publications

2004-08-16

Design and Control of Libration Point Spacecraft Formations

Infeld, Samantha I.; Josselyn, Scott B.; Murray, Walter; Ross, Michael I.

http://hdl.handle.net/10945/29650

Design and Control of Libration Point Spacecraft Formations

Samantha I. Infeld, * Scott B. Josselyn † Walter Murray, ‡ I. Michael Ross,§

We investigate the concurrent problem of orbit design and formation control around a libration point. The problem formulation is based on a framework of multi-agent, nonlinear optimal control. The optimality criterion is fuel consumption modeled as the L^1-norm of the control acceleration. Fuel budgets are allocated by isoperimetric constraints. The nonsmooth optimal control problem is discretized using DIDO, a software package that implements the Legendre pseudospectral method. The discretized problem is solved using SNOPT, a sequential quadratic programming solver. Among many, one of the advantages of our approach is that we do not require linearization or analytical results; consequently, the inherent nonlinearities associated with the problem are automatically exploited. Sample results for formations about the Sun-Earth L2 point in the 3-body circular restricted dynamical framework are presented. Globally optimal solutions for relaxed and almost periodic formations are presented for both a large separation constraint (about a third to half of orbit size), and a small separation constraint (a few hundred km or about 5×10^{-6} of orbit size).

I. Introduction

GIVEN the old adage that two or more persons working cooperatively can achieve more than the sum of their individual efforts, it is no surprise that the same holds for space systems. In fact, this concept holds for many other control systems such as underwater vehicles, mobile robots and airplanes including non-vehicular control systems such as those arising in medicine, economics and software engineering. Such multi-agent systems require a certain level of abstraction to manage complexity; see Tanner et al[1] for an excellent review of the literature and some recent results along this direction. A distributed space system (DSS) is a multi-agent control system and has long been recognized[2–5] as a key technology area to enhance the scope of both military[2, 4] and civilian[3, 5] space applications. A particular type of DSS that is challenging to design[2–5] is a collection of spacecraft in formation. Unlike other multi-agent systems, the design of a DSS has a specific unique requirement: the propellant consumption must be minimal.[4, 5] This requirement stems from the simple notion that if propellant consumption was not a prime driver, then any arbitrary configuration is possible, such as a circular "halo orbit" whose center is not the gravitating body in an inverse-square gravity field. Thus, to explore various formation configurations, it is crucial to concurrently design the formation and the minimum-fuel control.[6, 7] In other words, we do not necessarily propose to control a particular formation configuration in minimum fuel (i.e. the problem of optimal formation keeping); rather, we follow Ross et al[6] and King,[7] and propose that the more fundamental problem is to explore formation configurations (e.g. by varying initial estimates) that are minimum fuel solutions. Thus it is part of the method to find several locally optimal solutions, rather than looking for the one local optimal solution closest to an estimate of a particular formation configuration. Once this problem is solved, the next step would be to evaluate the formation configurations for science or military applications, modify the requirements if necessary, re-solve the problem and re-evaluate the result in conjunction with the propellant expenditures to determine its viability.[6] This approach, of telling agents what to do, rather than how to do it, has been successfully applied for the design and control of a variety of Earth-orbiting formations[6, 7] and station-keeping of libration-point missions.[12] In this paper, we extend the results of Infeld and Murray[12] by adopting the approach of Ross and King.[6, 7]

Research on formation at libration points is motivated primarily by the opportunity to create the effect of larger telescopes with a precise formation of smaller telescopes. Currently in design are infrared interferometry missions NASA's Terrestrial Planet Finder[8] and ESA's Darwin,[9] as well a NASA x-ray telescope formation mission, Constellation-X Observatory.[10] These are all located at the Sun-Earth L2 point. There are also ideas for formations spaced about a libration point orbit; more of a constellation around the point. An example of this idea is the two satellite constellation Solar Wind Satellite proposed at Sun-Earth L1 by the Department of Defense.[11] Similar to the extensive work on spacecraft formation in the two-body problem, much of the research on the

---

*Graduate Student, Stanford University. Student Member, AIAA.

†Research Assistant, LT, U. S. Navy

‡Professor, Stanford University

§Associate Professor, Naval Postgraduate School. Associate Fellow, AIAA.

Copyright © 2004 by the American Institute of Aeronautics and Astronautics, Inc. All rights reserved.

three-plus-body problem is centered around linearization about a reference libration orbit.[13–16] Thus, the problem is split into two problems: the design of a "good" reference orbit and formation control around the reference orbit. There are number of procedures for finding a reference orbit,[17,18] many of them are based on a Lindstedt-Poincaré technique proposed by Richardson.[19] In this approach, the perturbation method of Lindstedt is applied to the circular restricted three-body problem with Legendre polynomials as expansion coefficients. The accuracy of this method is then judged by comparing the results to a direct numerical integration of the dynamical equations. This naturally leads to a procedure for improving the initial conditions by shooting methods.[18,20] Junge et al[20] describe the issues and difficulties of this approach for real-life missions. Having determined the reference orbit in such a manner, formation keeping methodologies can be developed by applying linear control theory to the linearized equations of motion for a neighboring orbit.[15,16] Many variants of this approach are actively being pursued by various researchers. While such a two-step approach may be viable for certain missions, a simple, unified, single-step approach to the design and control of spacecraft formations was proposed by Ross and King.[6,7] In this approach, the orbits and the formation control strategies are designed concurrently using the framework of multi-agent optimal control theory. It will be apparent shortly that this framework, described Sec. II, is not the same as applying optimization techniques to compute the standard problem of impulsive trajectory correction maneuvers.[21] In any case, once the problem framework is set up, the optimal control problem it is solved by a Legendre pseudospectral method.[22–24] This method, summarized in Sec. III, essentially allows the state, control and costate variables to be represented as a series expansion of Legendre polynomials. Thus, although Legendre polynomials are also used, as in Richardson's method, the pseudospectral approach is fundamentally different and resembles a Galerkin method.[25] However, unlike a Galerkin method, all the computations in the pseudospectral method are performed in the time domain by an equivalent representation of the unknown variables in terms of Lagrange interpolating polynomials. The net result is that the semi-analytical framework of series expansion and the computational aspects of finding the coefficients are unified. The computational problem is reduced to a large nonlinear programming problem. Solving such large-scale problems are significantly easier today than ever before: thanks to major advances in practical algorithms pioneered by Betts[26] and Gill et al;[27] these algorithms promise global convergence under mild assumptions.[28] The results of this approach are reported in Sec. V. We briefly note that global convergence does not imply global optimality;[28,29] we also present

globally fuel-optimal solutions in the sense that the propellant expenditures are zero.

II. General Framework

A general framework for spacecraft formation design and control is described by Ross et al[6] and repeated here for the purposes of completeness. Suppose that we have a collection of $N_s \in \mathbb{N}$ spacecraft that constitute a DSS. Let $\mathbf{x}^i(t) \in \mathbb{R}^{N_{x^i}}$ denote the state of the ith spacecraft at time t. This can be the usual 6-vector position-velocity state or any other set (e.g. orbital elements). We assume that the dynamics of the DSS is given in some coordinate system by a set of differential equations,

$$\dot{\mathbf{x}}^i = \mathbf{f}^i(\mathbf{x}^i, \mathbf{u}^i, t; \mathbf{p}^i) \quad i = 1 \dots N_s, \qquad (1)$$

where $\mathbf{f}^i : \mathbb{R}^{N_{x^i}} \times \mathbb{R}^{N_{u^i}} \times \mathbb{R} \times \mathbb{R}^{N_{p^i}} \to \mathbb{R}^{N_{x^i}}$ is a given function, $\mathbf{u}^i \in \mathbb{U}^i \subseteq \mathbb{R}^{N_{u^i}}$ is the control variable of the ith spacecraft constrained to some compact set $\mathbb{U}^i$, and $\mathbf{p}^i \in \mathbb{R}^{N_{p^i}}$ is a vector of (constant) design parameters. In general, the dynamics need not be given in state-space form, as in Eq. (1), but for the purpose of brevity we limit our discussion to such a vector-field approach. By defining the state and control variables as,

$$\mathbf{x} = (\mathbf{x}^1, \dots, \mathbf{x}^{N_s}) \quad and \mathbf{u} = (\mathbf{u}^1, \dots, \mathbf{u}^{N_s}),$$

the dynamics of the DSS may be represented quite succinctly as,

$$\dot{\mathbf{x}} = \mathbf{f}(\mathbf{x}, \mathbf{u}, t; \mathbf{p}) \quad \mathbf{u} \in \mathbb{U}, \qquad (2)$$

where $\mathbb{U} = \mathbb{U}^1 \times \dots \times \mathbb{U}^{N_s}$. Typically, the functions $\mathbf{f}^i$ are all the same so that $\mathbf{f}$ is simply N_s copies of $\mathbf{f}^1$. Let $d(\mathbf{x}^i, \mathbf{x}^j) \in \mathbb{R}_+$ be a generic distance metric (not necessarily Euclidean) between any two spacecraft. If $d(\mathbf{x}^i(t), \mathbf{x}^j(t))$ is a given constant in time, $c^{i,j}$, then we say we have a ***frozen formation***,

$$c^{i,j} \leq d(\mathbf{x}^i(t), \mathbf{x}^j(t)) \leq c^{i,j} \qquad \forall\, t, i, j. \qquad (3)$$

Here and the rest of the paper, by $\forall\, t$, we mean for all t associated with the finite lifetime of the DSS whereas by $\forall\, i, j$ we mean $\forall\, i, j \in \{1, \dots, N_s\}$. Further, from the definition of a metric, $d(\mathbf{x}^i, \mathbf{x}^j) = 0 \,\forall\, i = j$; hence, we must have $c^{i,j} = 0 \,\forall\, i = j$ as a necessary condition for feasibility. Note that Eq.(3) is really an equality; the reason for masquerading it as an inequality is to define a ***relaxed formation*** as

$$c^{i,j} - \delta_l^{i,j} \leq d(\mathbf{x}^i(t), \mathbf{x}^j(t)) \leq c^{i,j} + \delta_u^{i,j} \qquad \forall\, t, i, j, \quad (4)$$

where $\delta_l^{i,j} \geq 0$ and $\delta_u^{i,j} \geq 0$ are lower and upper tolerances associated with the relaxation. When $i = j$, the tolerances must be zero in conformance with the definition of a metric. Equation (4) generalizes Eq.(3) since if $\delta_l^{i,j} = \delta_u^{i,j} = 0 \,\forall\, i, j$, we recover the representation of the frozen formation defined by Eq.(3).

We can define and design various configurations based on various metrics. For example, in libration point missions, in order to generate halo orbits, there may be a forbidden zone such as a disk of radius R centered around the libration point, $\mathbf{y}$; in this case, we define an allowable region for $\mathbf{x}$ as,

$$d(\mathbf{x}^i(t), \mathbf{y}) \geq R \qquad \forall\ i, t.$$

See King[7] for an implementation of such constraints for a variety of Earth-orbiting missions. The requirement that no two spacecraft collide may be articulated as,

$$d(\mathbf{x}^i(t), \mathbf{x}^j(t)) \geq b^{i,j} > 0 \qquad \forall\ t \text{ and } i \neq j.$$

It is apparent that all these constraints (and many more that are specific to a particular mission) can be described in terms of a generic set of a possibly large number of inequality constraints that can be represented as,

$$\mathbf{h}_l \leq \mathbf{h}(\mathbf{x}, \mathbf{u}, t; \mathbf{p}) \leq \mathbf{h}_u, \tag{5}$$

where $\mathbf{h} : \mathbb{R}^{N_x} \times \mathbb{R}^{N_u} \times \mathbb{R} \times \mathbb{R}^{N_p} \to \mathbb{R}^{N_h}$ and $\mathbf{h}_l, \mathbf{h}_u, \in \mathbb{R}^{N_h}$. In this description of a formation, there is no leader or follower; rather a system of multiple spacecraft. Thus, if any one spacecraft has an additional configuration constraint, it would automatically transfer in some fashion to the remainder of DSS by way of the couplings between the various equations. For example, if there was a mission requirement to designate a particular spacecraft as a leader and designate the others as followers, this can be easily accomplished by picking out the particular index, i, representing the leader. Then, when the leader moves along some trajectory, $t \mapsto \mathbf{x}^i$, the distance metrics along with any additional path constraints, Eq.(5), dictate how the remainder of the spacecraft must follow certain trajectories to meet the path constraints; i.e., a formation. Thus, although our framework is based on a collection of DSS, it does not exclude a leader-follower system.

As noted earlier, fuel consumption dominates any DSS design. Since L^1-norms are a direct measure of fuel expenditures,[30] we compute the fuel consumption for any one spacecraft, i, according to,

$$J_i = \int_{t_0}^{t_f} \left\| \mathbf{u}^i(t) \right\|_1 \, dt, \tag{6}$$

where $t_f - t_0$ is the time interval of interest and $\|\cdot\|_1$ is the usual l^1-norm. Note that the cost function is non-smooth[31] and represents a practical configuration of six thrusters.[30] The whole discretized system is a well-posed smooth problem because of the use of six thrusters, because each is positive and bounded by zero. The reason for not choosing the more popular smooth quadratic cost is that the L^2-norm of the control does not minimize propellant expenditures.[30] Treating the problem to be invariant under time translations allows us to set $t_0 = 0$. A critical modeling

issue in the design and control of spacecraft formations is the treatment of the horizon, t_f, vis-à-vis the mission life time. Ideally, we would like to choose t_f to be equal to the mission life. Deferring a discussion of alternative choices for the horizon, we choose the cost functional for designing the DSS to be the total fuel consumption,

$$J = \sum_{i=1}^{N_s} J_i = \int_{t_0}^{t_f} \sum_{i=1}^{N_s} \left\| \mathbf{u}^i(t) \right\|_1 \, dt. \tag{7}$$

In certain applications, it may be necessary to require that each spacecraft in the DSS consume the same amount of propellant. This requirement can be stipulated as the so-called isoperimetric constraints,

$$J_i = J_k \quad \forall\ i, k. \tag{8}$$

If the equal-fuel requirement is "soft" as in, $J_i \approx J_k$, it can be simply stipulated as an inequality with appropriate upper and lower bounds. Likewise, the allocation of fuel budgets can be similarly defined.

It will be apparent shortly that the problem formulation as posed so far is quite sufficient to handle Libration point formations in the Sun-Earth system if the spacecraft lifetime measured in terms of the duration of the formation is about a year or so as in the Genesis Mission.[32] This is because the number of halo orbits over this duration is about two. For a similar lifespan, the number of orbits in the two-body Earth system range from several hundred to thousands. To properly account for this periodicity, we adapt Bohr's notion of almost periodic functions.[33, 34] Under this framework,[6, 35] periodicity may be exploited for an alternative problem formulation based on a modification to optimal periodic control theory. In this problem formulation, we write[6, 35]

$$J = \frac{1}{t_f - t_0} \int_{t_0}^{t_f} \sum_{i=1}^{N_s} \left\| \mathbf{u}^i(t) \right\|_1 \, dt, \tag{9}$$

which is a measure of fuel consumed by the DSS averaged over the time period, $(t_f - t_0)$. It is quite tempting to choose *a priori* this time period equal to the period of some appropriately chosen reference orbit; however, a far better option[6] is to let this period be free so that the problem formulation allows the determination of an optimal time period as well. In this case t_f is bound away from t_0 to prevent invalid function evaluations. As noted in Sec. I, this option tells the agents what to do rather than how to do it. In order to facilitate the existence of a solution for this scenario, it is now necessary to impose two additional constraints on the problem formulation:

1. The dynamical equations, Eq.(1), must be written in an appropriate coordinate system that facilitates a periodic or almost periodic solution, and

2. Boundary conditions representing the almost periodic structure of the desired solution must be included.

Thus, assuming that the the first condition is satisfied, the boundary conditions for strict periodicity of a **periodic formation** can be stipulated as,

$$\mathbf{x}^i(t_0) = \mathbf{x}^i(t_f) \quad \forall\, i. \tag{10}$$

Two points are worth noting at this juncture: first, these conditions are not the same as specifying standard boundary conditions because the values of $\mathbf{x}^i(t_0)$ and $\mathbf{x}^i(t_f)$ are unknown. Second, as briefly noted earlier, it is sufficient to stipulate all the constraints of Eq.(10) as a single constraint,

$$\mathbf{x}^i(t_0) = \mathbf{x}^i(t_f) \quad \text{for} \quad i = 1 \tag{11}$$

or any other index. This is because, the path constraints will automatically enforce the remainder of the constraints. In this context, we may designate $i = 1$ as the leader, but it essentially reduces to semantics rather than a leader-follower architecture. By relaxing the constraint represented by Eq(10) to,

$$\varepsilon_l^i \leq \mathbf{x}^i(t_0) - \mathbf{x}^i(t_f) \leq \varepsilon_u^i \quad \forall\, i, \tag{12}$$

where ε_l^i and ε_u^i are formation design parameters, we easily stipulate a practical means to design and control almost periodic formations.[7] It is clear from these definitions that a frozen formation in the Euclidean metric is a periodic formation but not vice versa. The concept of almost periodicity is not only quite practical, it has significant theoretical advantages. See Fischer[33] for a quick review of almost periodic functions, and Junge et al[20] for practical demonstrations of possible contradictions in applying ordinary Floquet analysis. Deferring the details of applying this framework for Libration point missions to Sec. IV, we note that the problem of designing and controlling spacecraft formations can be summarized as a nonsmooth, nonlinear, multi-agent optimal control problem.

III. Solving Multi-Agent Optimal Control Problems

Solving multi-agent optimal control problems are, in principle, more complicated than ordinary optimal control problems. Until about the early 1990s, solving even a smooth nonlinear optimal control problem was widely considered to be extremely difficult. As noted in Sec. I, rapid advances in globally convergent computational methods have altered our notion of difficult and easy problems. In his famous statement, Rockafellar[36] noted that, "... the great watershed in optimization isn't between linearity and nonlinearity, but convexity and nonconvexity." Until the late 1990s, advancements in optimization did not translate to advancements in optimal control since discretization and
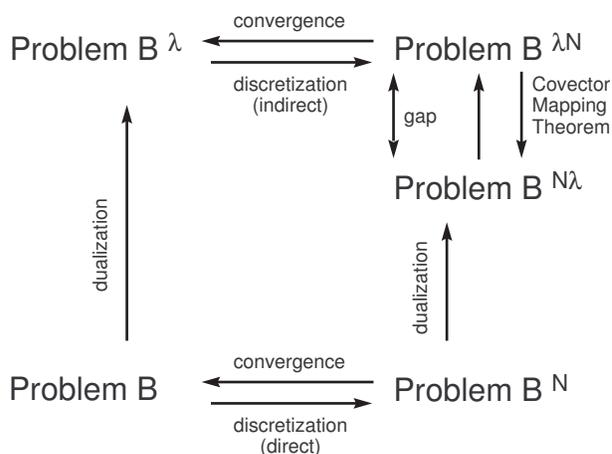

Fig. 1 Solving optimal control problems (from Ross and Fahroo[23, 29])

dualization are noncommutative operations.[29] Thus, a Runge-Kutta method that converges for ordinary differential equations may fail gloriously when applied to optimal control problems.[37] When a proper discretization is blended with modern algorithms, not only does it render "difficult problems" easy, it also enlightens why one approach is unquestionably superior to another as amplified by Betts et al.[38] Much of the technical issues pertaining to solving optimal control problems can be encapsulated by the diagram shown in Fig. 1.

Let Problem B denote a generic Bolza optimal control problem; then, Problem B^λ represents the primal-dual boundary value problem obtained by applying the Minimum Principle. Much of the difficulties reported in the literature center around solving Problem B^λ. Regardless of the type of method applied to solving Problem B^λ, the sheer act of using a computer to solve it implies discretization: this is denoted abstractly as Problem $B^{\lambda N}$ to denote that a computational solution is sought after dualization, where N denotes some degree of approximation. Problem $B^{\lambda N}$ is fundamentally difficult to solve due to a variety of reasons that goes to the heart of the symplectic structure of Hamiltonian systems and numerical propagation.[39] The simpler path to solve optimal controls problems is to discretize first (Problem B^N in Fig. 1) and dualize afterwards.[26, 29, 38] Solving an optimal control problem is fundamentally different from numerical propagation of an ordinary differential equation: the former is a global problem while the latter is local problem. Thus, even traditional methods for convergence analysis must be abandoned in favor of new ideas.[37, 38] The implementation of these ideas require that any gap (see Fig. 1) resulting in favor of discretizing prior to dualizing must be closed, if it can be closed at al. Thus, if a discretization based on the popular family of Runge-Kutta methods is desired, the correct approach

for solving optimal control problems is the Hager family of Runge-Kutta methods.[37, 40]

In recent years, pseudospectral (PS) methods have been widely applied to solve optimal control problems. See the recent paper by Ross and Fahroo[24] and the references contained therein. PS methods satisfy conditions similar to those of the Runge-Kutta-Hager method but offer higher accuracy known as spectral accuracy.[41] To truly appreciate this concept in the context of optimal control, we use the notion of a Sobolev space.[42] See Ross[30] for a practical demonstration of the utility of Sobolev spaces. A Sobolev space, denoted as, $W^{m,p}(\Omega, \mathbb{R})$, consists of all functions, $f : \mathbb{R} \supseteq \Omega \to \mathbb{R}$ whose jth-derivative is in L^p for all $0 \le j \le m$. The Sobolev norm of f is defined as,

$$\|f\|_{W^{m,p}} := \sum_{j=0}^{m} \left\| f^{(j)} \right\|_{L^p}. \tag{13}$$

This definition implies that the normed space $W^{0,p}$ is the same as L^p. The integer, m, is essentially a mathematical representation of smoothness. This concept allows us to state the following informal theorem[43]

Theorem 1.1 (Convergence) *Let* $\mathbf{x}^*(\cdot)$ $\in$ $W^{m_x,\infty}([\tau_0, \tau_f], \mathbb{R}^{N_x})$ *be the optimal state trajectory associated with the optimal control trajectory,* $\mathbf{u}^*(\cdot) \in W^{m_u,\infty}([\tau_0, \tau_f], \mathbb{R}^{N_u})$. *Under proper technical conditions, the following convergence result holds*

$$\left\| \mathbf{x}^*(\cdot) - \mathbf{x}^N(\cdot) \right\|_{L^\infty} = O(N^{-m_x})$$
$$\left\| \mathbf{u}^*(\cdot) - \mathbf{u}^N(\cdot) \right\|_{L^\infty} = O(N^{-m_u}).$$

From this theorem it is clear that the smoother the optimal solution, the faster the convergence of the PS solution. Moreover, the Covector Mapping Theorem[23, 29](see Fig. 1) allows a quick check of the satisfaction of the optimality conditions without an explicit derivation of the all the necessary conditions that can be quite burdensome in solving practical problems.[26] Thus the multi-agent problem posed in Sec. II can be solved quite readily. The PS method is implemented in DIDO[44] within the MATLAB problem solving environment. No explicit knowledge of PS methods or nonlinear programming techniques is necessary to use DIDO. The software exploits the suite of mathematical programming solvers available through TOMLAB.[45] The default solver in DIDO is SNOPT.[27]

As a matter of completeness we note that any real-time computational scheme automatically implies a feedback implementation.[30] For orbit control applications, the goals of real-time computation can be met if the computation time is significantly less than the orbital period (relative orbit for formation keeping). This is the well-known concept of a sampled-data feedback system. Given that halo orbital periods for the Sun-Earth system is about 180 days, if a computational method took as large as one day to compute a
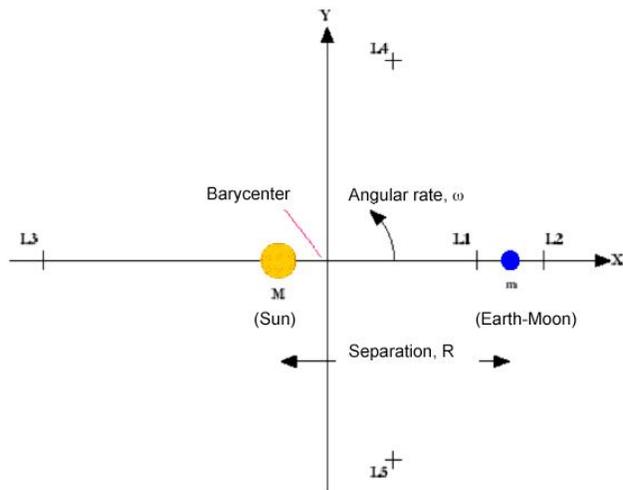
Fig. 2 Coordinate system for the restricted three-body problem

solution, it would generate 180 samples per orbit. In other words, solutions obtained in a matter of hours can also be interpreted as a one-sample feedback solution. Depending upon the problem, PS methods have been demonstrated to produce solutions in fractions of a second[43, 46–48] that include a starting point from random guesses.[46] Thus, if an optimal control problem can be formulated, modern methods can be used to generate "robust" solutions in real-time for a wide variety of problems. The multi-agent problem posed in Sec. II belongs to this family of solvable problems. We note that not all multi-agent problems can be posed under the framework of Sec. II; for example, the multi-agent launch problem[49] can only be posed as a hybrid optimal control problem involving categorical variables.[50]

IV. Libration Point Formations

Let $\mathbf{r}^i = (x^i, y^i, z^i)$ denote the Cartesian components of a generic spacecraft in the barycentric frame (see Fig. 2) of the circular restricted three-body problem. The spacecraft dynamical equations are well-known and given by,

$$\dot{\mathbf{r}}^i = \mathbf{v}^i \tag{14}$$
$$\dot{\mathbf{v}}^i = \mathbf{C}\mathbf{v}^i + \frac{\partial U^i}{\partial \mathbf{r}^i} + \mathbf{u}^i, \tag{15}$$

where

$$\mathbf{C} = \begin{pmatrix} 0 & -2 & 0 \\ 2 & 0 & 0 \end{pmatrix}$$
$$U^i \equiv U(x^i, y^i, z^i)$$
$$U(x, y, z) = \frac{x^2 + y^2}{2} + \frac{1-\mu}{r_A(x,y,z)} + \frac{\mu}{r_B(x,y,z)}$$
$$r_A^2(x,y,z) = (x + \mu)^2 + y^2 + z^2$$
$$r_B^2(x,y,z) = (x + \mu - 1)^2 + y^2 + z^2.$$

The acceleration control $\mathbf{u}^i$ is norm-bounded,

$$\left\| \mathbf{u}^i \right\|_\infty \leq u^i_{max}$$

and represents the thruster size of a particular configuration.[30] A multitude of formation options can be defined in various ways. For example, it may be necessary to keep the relative Euclidean distance (l^2-norm) bounded according to,

$$c_2^{i,j} - \delta_l^{i,j} \leq \left\| \mathbf{r}^i(t) - \mathbf{r}^j(t) \right\|_2 \leq c_2^{i,j} + \delta_u^{i,j} \qquad \forall\, t, i, j \tag{16}$$

Another option may require to bound the l^∞-norm,

$$c_\infty^{i,j} - \delta_l^{i,j} \leq \left\| \mathbf{r}^i(t) - \mathbf{r}^j(t) \right\|_\infty \leq c_\infty^{i,j} + \delta_u^{i,j} \qquad \forall\, t, i, j \tag{17}$$

as an alternative or additional requirement. In some complex mission geometries, metrics not based on norms may also be used. All the conditions posed above apply to relative formation configurations. In order to design the ensemble about a generic Lagrange point, $L \in \{L1, \ldots, L5\}$, an allowable zone can be defined as,

$$c_l^{i,L} \leq \left\| \mathbf{r}^i(t) - \mathbf{r}_L \right\|_2 \leq c_u^{i,L} \qquad \forall\, t, i,$$

where $\mathbf{r}_L$ is the position vector of L. Similar to the relative configuration metrics, other metrics or norms may also be chosen for the allowable zone.

All of the prior conditions apply to a design of the formation system. Thus there is no leader or follower system; rather a system of distributed spacecraft. As noted before, it is possible to transmit conditions to the entire system by stipulating conditions on any one spacecraft. For example, to create a formation along a halo orbit, it is necessary to specify the "halo conditions" for just one spacecraft. This is also an orbit design problem and can be designed concurrently with the formation by imposing additional conditions. For example, if the formation system is required to be periodic, then it is necessary to impose the periodic conditions for just one spacecraft, say

$$\mathbf{r}^j(t_0) = \mathbf{r}^j(t_f) \tag{18}$$
$$\mathbf{v}^j(t_0) = \mathbf{v}^j(t_f) \quad \text{for } j = 1. \tag{19}$$

To generate almost periodic trajectories, these conditions can be relaxed to give

$$\varepsilon_{r,l}^j \leq \mathbf{r}^j(t_0) - \mathbf{r}^j(t_f) \leq \varepsilon_{r,u}^j \tag{20}$$
$$\varepsilon_{v,l}^j \leq \mathbf{v}^j(t_0) - \mathbf{v}^j(t_f) \leq \varepsilon_{v,u}^j \quad \text{for } j = 1. \tag{21}$$

V. Numerical Examples

We demonstrate our ideas for a two spacecraft system ($N_s = 2$); the extension of this approach to three or more spacecraft is straightforward. Although our method can be applied to any libration point with similar results, we choose to design and control formations about the Sun-Earth $L2$ point because of the multitude of telescope formation missions proposed at this location; thus, we have,

$$\mu = 2.448 \times 10^{-6}$$
$$\mathbf{r}_L = (1 - \mu + 0.01, 0, 0)\ DU$$

in the barycentric frame, where DU is the distance unit equal to the astronomical unit, AU. The origin in these examples is shifted to $L2$ to improve variable scaling, so $\mathbf{r}_L = (0, 0, 0)$. Also, we chose the Euclidean distance, the maximum acceleration and the allowable zone parameters as the design parameters. The separation parameter between the two spacecraft is chosen to reflect the spread of an interferometry mission. The TPF requirement is a 1km range (see requirements in Ref.[8]). The next generation of "hypertelescopes" being explored by optical engineers[51] will use even larger baselines for resolution of smaller objects. At 150 km, characteristics of Earth-sized planets several parsecs away can be directly observed. At one million km, the hypertelescope will angularly resolve neutron stars, which are hundreds of parsecs away. We choose 15 km as the separation for our first two examples. In problem formulations with constraint dimensions this small in comparison to the state variable size (4 orders of magnitude difference), issues of scaling must be resolved in order to obtain optimal solutions. In the last example, the separation is much larger, approaching one million km, which reflects the design of a constellation of observers, similar to the SWS proposal (in Ref.[11]), or the outer edges of the DSS neutron star observer of the distant future.

Example 1

In the first example, we consider a fixed-horizon problem, and set $t_f = 3.5\ timeunits(TU)$ (about 205 days). The time unit is equal to the period of the rotation system, which is the inverse of the frequency, 2π radians per year. In seeking a relaxed formation with a separation of 1×10^{-7} DU (about 15 km), we set the design parameters as,

$$c_2^{i,j} = 1 \times 10^{-7}\ DU \ \text{ for } i \neq j \tag{22}$$
$$\delta_2^{i,j} = 5 \times 10^{-6}\ DU \ \text{ for } i \neq j \tag{23}$$
$$u^i_{max} = 0.001\ DU/TU^2\ \forall\, i \tag{24}$$
$$J_i = J_k \quad \forall\, i, k, \tag{25}$$

where TU, the time unit is $1/(2\pi)$ of the period of the of the primary system; i.e. a year for the Sun-Earth system. The input states and controls (the starting point for the optimization algorithm) were found by propagating an initial state and applying enough thrust along the x axis at the step closest to crossing the $x - z$ plane to make the x velocity zero at the next step. This was done for 3 maneuver and propagate cycles, producing a trajectory tracing a little further than one "orbit", and a final time of 3.5 TU (thus the

t_f defined above). This set of states and controls are the input for both spacecraft. This means the initial estimate of the solution is infeasible since the separation is below the minimum bound. The initial state that produced the input for this example is (in DU and DU/TU):

$$
\begin{aligned}
x(t_0) &= 0.0 \times 10^{-3}, & v_x(t_0) &= 1.0 \times 10^{-3} \\
y(t_0) &= 2.5 \times 10^{-3}, & v_y(t_0) &= -4.5 \times 10^{-3} \\
z(t_0) &= 1.0 \times 10^{-3}, & v_z(t_0) &= -1.0 \times 10^{-3}
\end{aligned}
$$

To reduce the computation time, the initial state of the solution was bound to a box of 0.001 *DU* on either side of the about input initial state. Periodic constraints are not imposed but the isoperimetric constraint of equal-fuel consumption is required (Cf. Eq. (25)). As noted earlier, we used DIDO[44] with SNOPT[27] to solve the multi-agent optimal control design problem. A solution to the problem for a choice of 100 nodes (roughly, a 99th-order Legendre polynomial) is shown in Fig. 3. This solution is globally optimal because it has zero cost, i.e. $J = 0 \Leftrightarrow \mathbf{u} = \mathbf{0}$. The trajectories
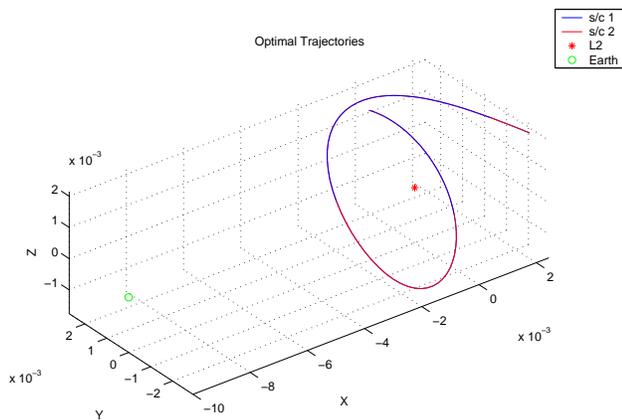
Fig. 3 Trajectories for a two-agent DSS

show that each of the two spacecraft appear to follow the same shaped halo-like orbit about L2, but parallel along the path, maintaining the tolerances on the specified separation distance as shown in Fig. 4. The relative orbit, i.e. the orbit of one of the spacecraft relative to the other, is shown in Fig. 5. The optimal controls are all zero at each node as shown in Fig. 6. The plots for the other thrusters are similar.

Our claim of optimality is based on several tests as described in Ref.[44]. One of these tests is the approximate constancy of the Hamiltonian with an average value equal to zero.[23] The non-zero values of the Hamiltonian for this example are trivially small as shown in Fig. 7. In order to practically demonstrate the convergence of the solution, we use the optimal
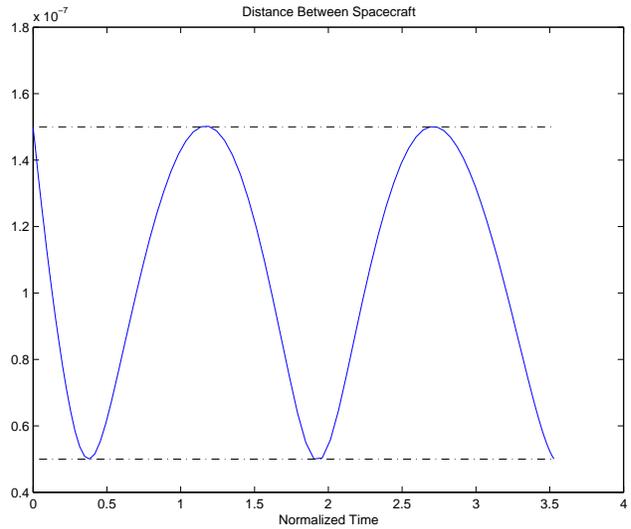

Fig. 4 Separation between the two spacecraft over time
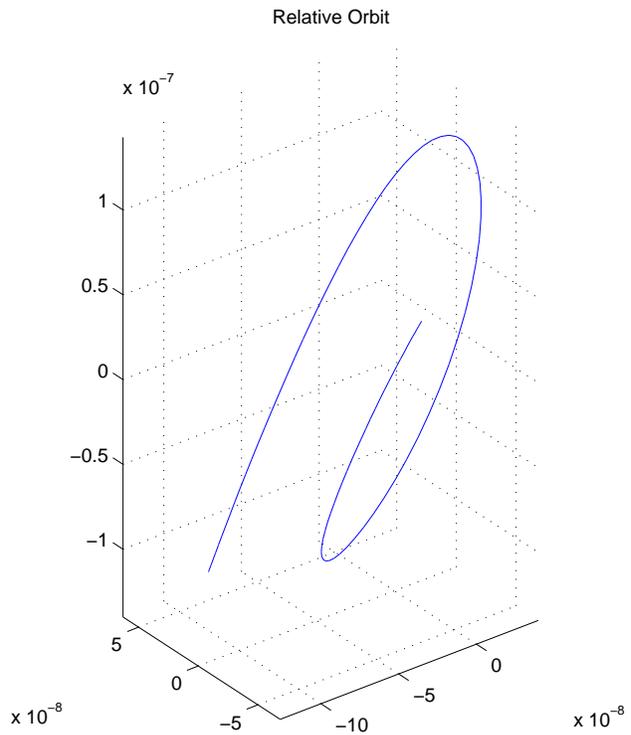
Fig. 5 Relative orbit for the two-agent DSS

initial conditions (in DU and DU/TU),

$$
\begin{aligned}
x^1(t_0) &= -0.43 \times 10^{-3}, & v_x^1(t_0) &= 2.00 \times 10^{-3} \\
y^1(t_0) &= 1.52 \times 10^{-3}, & v_y^1(t_0) &= -4.30 \times 10^{-3} \\
z^1(t_0) &= 1.93 \times 10^{-3}, & v_z^1(t_0) &= -0.15 \times 10^{-3}
\end{aligned}
$$

($\mathbf{x}^2(t_0)$ is the required $1 \times 10^{-7} DU$ away in position, and has similarly small differences in velocity) to propagate the solutions using ode45 in MATLAB. Fig. 8 shows a comparison of the optimized states to the
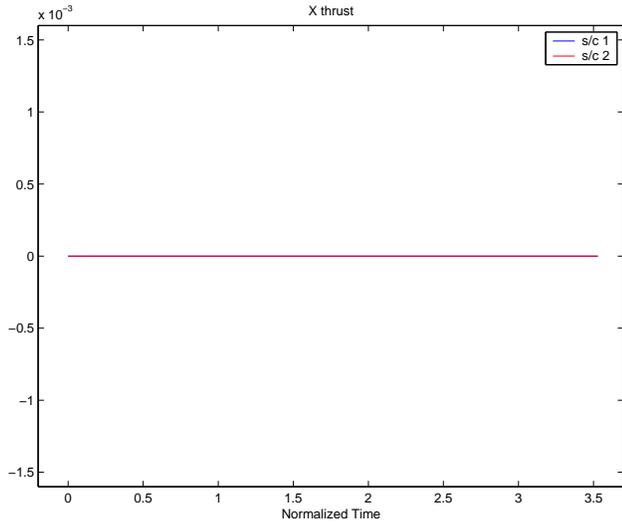
**Fig. 6   Thrust along the x axis for the two-agent DSS**
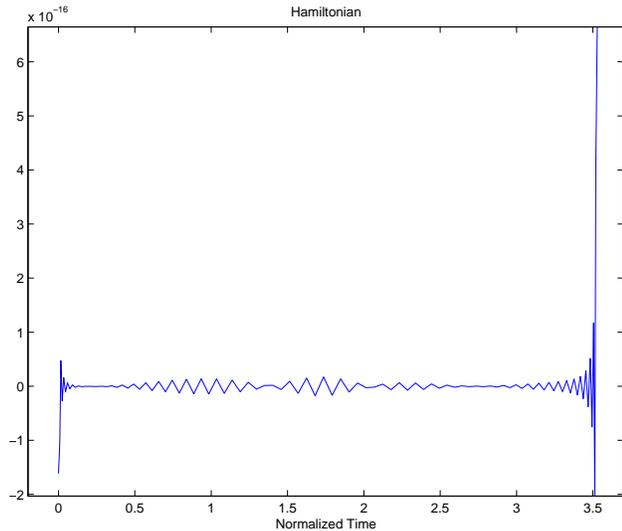
Fig. 7   Evolution of the Hamiltonian for the two-agent DSS; note the scale on the ordinate

propagated states of one of the spacecraft. It is apparent that the propagated states track fairly well to the optimized ones indicating that the 100 node solution is a good solution over this time period for preliminary design considerations. The timestep at which the solution diverges from the propagated trajectory increases proportionally to the number of nodes.

Example 2

Having obtained a zero-cost solution in Example 1, we now consider the same problem with the addition of periodicity constraints. As explained in Sec. II, periodicity in the states is imposed under a free horizon,
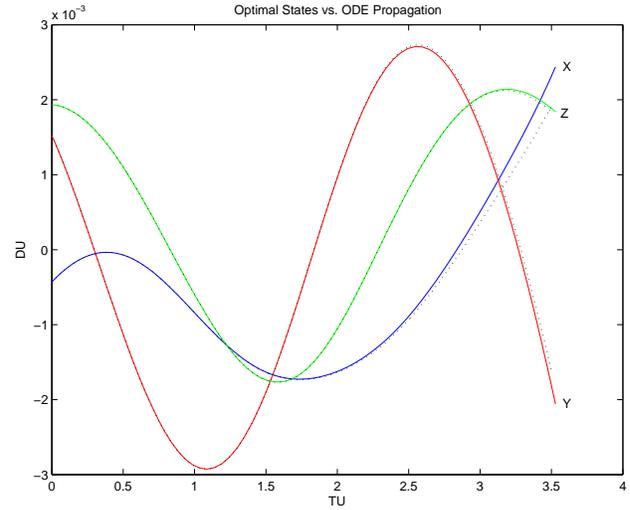
Fig. 8   Comparison of the position states of spacecraft one (solid) to those propagated by ODE45 in Matlab (dotted)

t_f; thus, we now have,

$$
\begin{align}
c_2^{i,j} &= 1 \times 10^{-7} \ DU \ \text{ for } i \neq j \tag{26}\\
\delta_2^{i,j} &= 5 \times 10^{-6} \ DU \ \text{ for } i \neq j \tag{27}\\
u_{max}^i &= 0.001 \ DU/TU^2 \ \forall \ i \tag{28}\\
J_i &= J_k \quad \forall \ i,k \tag{29}\\
\mathbf{x}^i(t_0) &= \mathbf{x}^i(t_f) \quad \text{for} \ i = 1. \tag{30}
\end{align}
$$

The input states and controls for this example were the optimal states and controls of the first example. The initial state of the solution was again bound to a box of 0.001 DU on either side, but only the positions were bound so that the initial velocities were totally free variables. This input trajectory is shown along with the optimal trajectories in Fig. 10, which is a zoomed in and stetched view of Fig. 9 Nevertheless, the trajectory plots illustrate that the solution to this problem is substantially different from that of Example 1. To properly illustrate the shape of this orbit, the trajectory in y-z plane is plotted in Fig. 11 with y-axis stretched appropriately.   The optimal period, t_f, for this design configuration was 3.18 TU, or 185 days. This solution is also globally optimal because $J \approx 0$. That $\mathbf{u}$ is almost zero (well within numerical tolerances) is shown in Fig. 12 for one of the thrusters. The plots for the other thrusters are similar.

The trajectories show that each of the two spacecraft appear to follow the same orbit about L2, but parallel along the path, maintaining the tolerances on the specified separation distance as shown in Fig. 13.

The relative orbit is shown in Fig. 14. A clearer picture of the satisfaction of the periodicity constraints is illustrated in Fig.s 15 and 16. The circles in Fig. 15 are the initial and final (x, y, z). In Fig. 16 they mark the initial and final (v_x, v_y, v_z). The velocity plot shows only the data for spacecraft one for clarity. Of course,
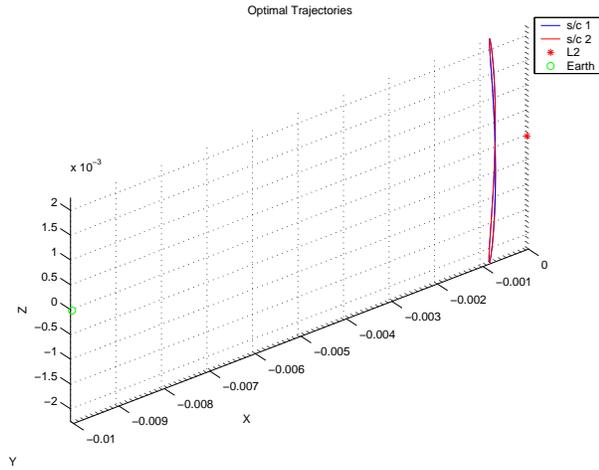
Fig. 9   Trajectories for a two-agent DSS with periodicity constraints
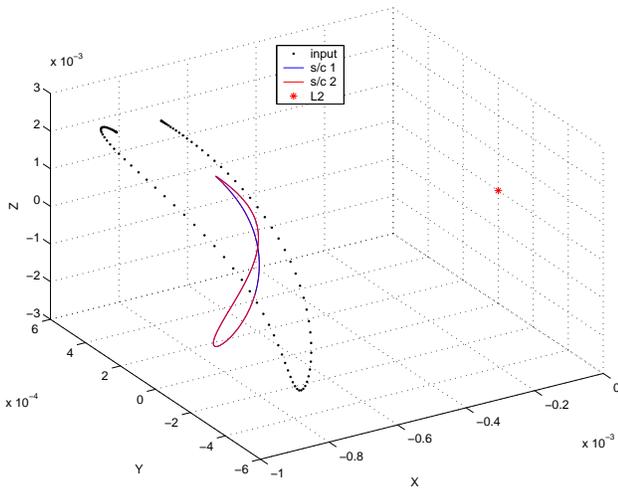
Fig. 10   Input and Optimal Trajectories for a two-agent DSS with periodicity constraints. NOT TO SCALE: stretched to show orbit shape

$\mathbf{x}^i(t_0)$ does not exactly equal $\mathbf{x}^i(t_f)$, but the differences are all around 1×10^{-7} DU, with the largest difference occurring in the z velocities of 2×10^{-6} DU. These are physically small enough compared to the orbital dimension of about 0.002 DU to confirm that the set feasibility tolerances for the optimization algorithm make sense.

The Hamiltonian plot in Fig. 17 shows that this is an optimal solution because of its average value of zero.

We demonstrate the convergence of this large-baseline solution by propagating a trajectory from the optimal initial conditions (in DU and DU/TU),

$$
\begin{aligned}
x^1(t_0) &= -0.78 \times 10^{-3}, & v_x^1(t_0) &= 0.23 \times 10^{-3} \\
y^1(t_0) &= 0.03 \times 10^{-3}, & v_y^1(t_0) &= 0.05 \times 10^{-3} \\
z^1(t_0) &= 1.86 \times 10^{-3}, & v_z^1(t_0) &= -2.53 \times 10^{-3}
\end{aligned}
$$

($\mathbf{x}^2(t_0)$ is the required $1 \times 10^{-7} DU$ away in position,
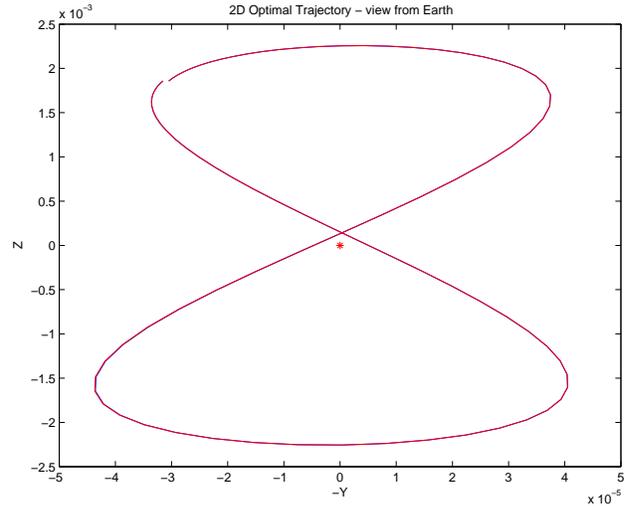
Fig. 11   Trajectories on the y-z plane for a two-agent DSS with periodicity constraints. NOT TO SCALE: stretched along the y axis
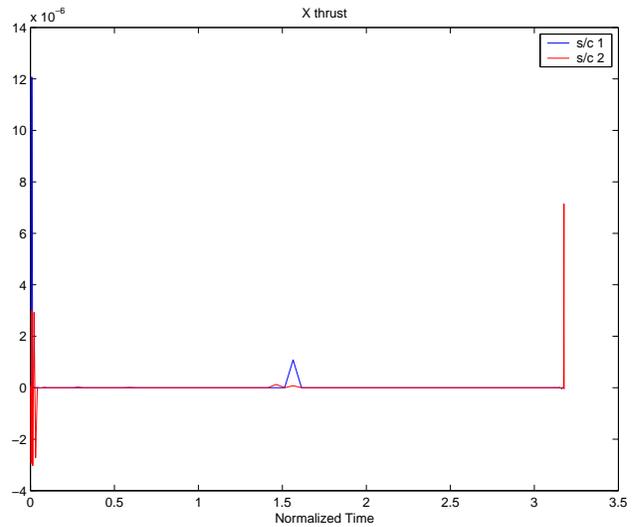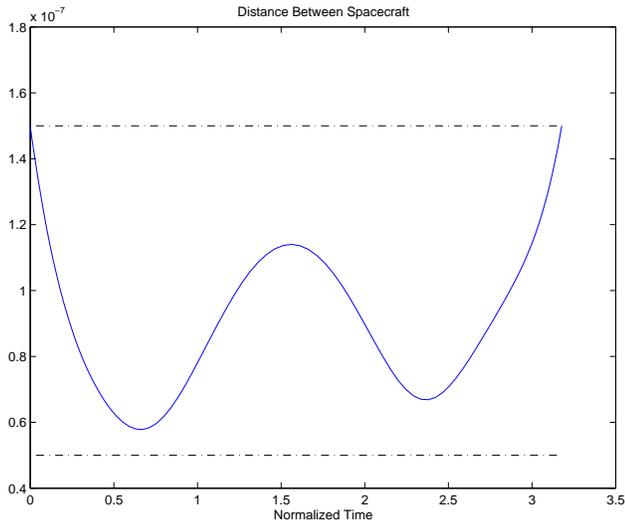

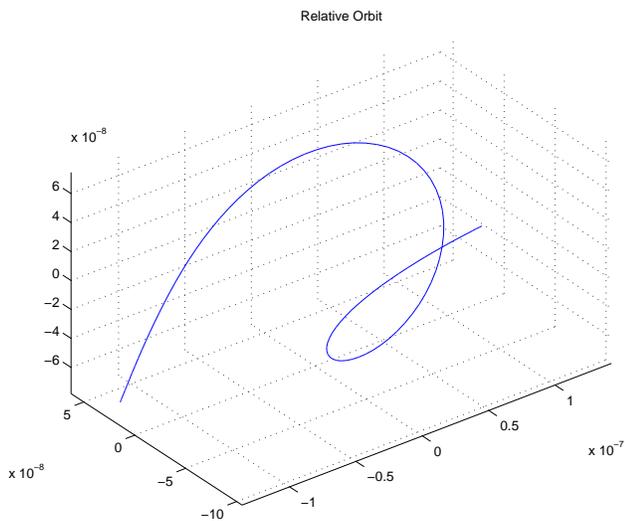**Fig. 12   Thrust along the x axis for the periodic two-agent DSS.**

and has similarly small differences in velocity), using `ode45` in MATLAB. Fig. 18 shows a comparison of the optimized states to the propagated states of one of the spacecraft. It is apparent that the propagated states track fairly well to the optimized ones indicated that the 100 node solution is a good solution for preliminary design considerations.

Example 3

In this example, we are looking for a large baseline formation, with spacecraft spread out over the libration point orbital space. This kind of formation would be used for the constellation type of mission, like the Solar Wind Satellite mentioned in Section I. Thus we want a separation of about one third to one half of the 'diameter' of the orbit, which from previous experiments with orbits found using the same input is about

Fig. 13 Separation between the two spacecraft over time

Fig. 15   The values of the position half of $\mathbf{x}^i(t_0)$ and $\mathbf{x}^i(t_f)$ for $i = 1, 2$ are marked with circles on this close-up view of the trajectory where it starts and ends.

Fig. 14   Relative orbit for the periodic two-agent DSS
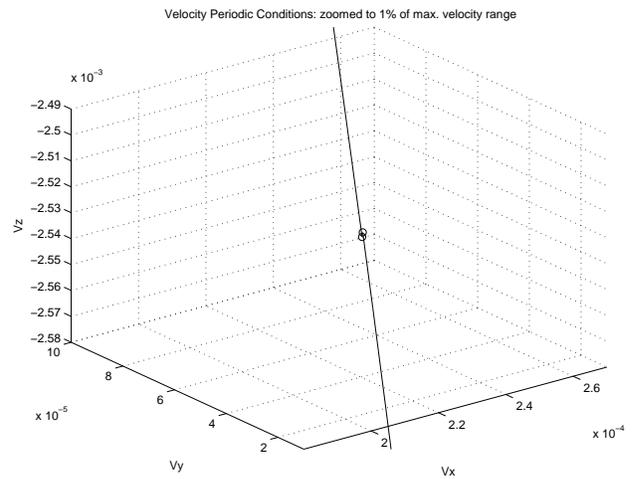
Fig. 16   The values of the velocity half $\mathbf{x}^i(t_0)$ and $\mathbf{x}^i(t_f)$ for $i = 1$ are marked with circles on this close-up view of the velocity trajectory start and end.

.005 DU; around 750,000 km. The nominal values of the design parameters for the third example are,

$$c_2^{i,j} = 0.002 \ DU \ \text{ for } i \neq j \qquad (31)$$

$$\delta_2^{i,j} = 0.0015 \ DU \ \text{ for } i \neq j \qquad (32)$$

$$u_{max}^i = 0.001 \ DU/TU^2 \ \forall \ i. \qquad (33)$$

The input states and controls are those of the first example, a propagation and maneuver schedule starting from the same initial state. The horizon, t_f was fixed then at 3.5 TU . No periodicity constraints were imposed, and the initial states were all free with no bounds, however there were bounds on the positions of $\pm 5 \times 10^{-3}$, which was an active constraint at a few time steps for the x coordinate.

A solution to the problem for the choice of parameters listed above is shown in Fig. 19. This solution

again is globally optimal because it has zero cost, i.e. $J = 0 \Leftrightarrow \mathbf{u} = \mathbf{0}$. The trajectories show that each of the two spacecraft appear to follow distinct halo-like orbits about L2 maintaining the tolerances on the specified separation distance as shown in Fig. 21. The relative orbit, i.e. the orbit of one of the spacecraft relative to the other, is more illustrative of the configuration and is shown in Fig. 22.

The Hamiltonian plot in Fig. 23 shows that this is an optimal solution because of it's average value of zero. We demonstrate the convergence of this large-baseline solution by propagating a trajectory from the optimal
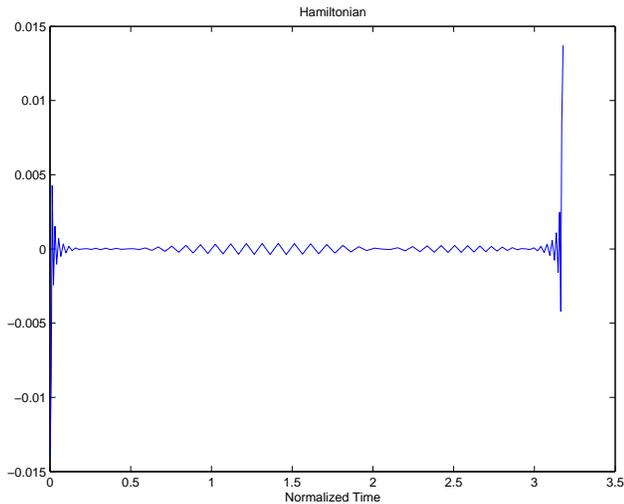
**Fig. 17   Evolution of the Hamiltonian for the periodic two-agent DSS**
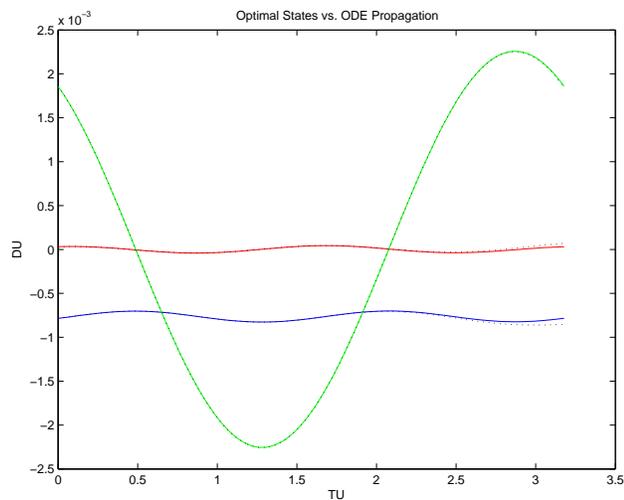
Fig. 18   Comparison of the position states of spacecraft one (solid) to those propagated by ODE45 in Matlab(dotted)

initial conditions (in DU and DU/TU),

$$
\begin{aligned}
x^1(t_0) &= -5.00 \times 10^{-3}, & x^2(t_0) &= -3.94 \times 10^{-3} \\
y^1(t_0) &= 1.94 \times 10^{-3}, & y^2(t_0) &= 0.71 \times 10^{-3} \\
z^1(t_0) &= 2.72 \times 10^{-3}, & z^2(t_0) &= 2.09 \times 10^{-3} \\
v_x^1(t_0) &= 12.74 \times 10^{-3}, & v_x^2(t_0) &= 10.55 \times 10^{-3} \\
v_y^1(t_0) &= 3.50 \times 10^{-3}, & v_y^2(t_0) &= -2.30 \times 10^{-3} \\
v_z^1(t_0) &= 7.88 \times 10^{-3}, & v_z^2(t_0) &= 10.54 \times 10^{-3}
\end{aligned}
$$

(note $\mathbf{x}^2(t_0)$ is the required distance away from $\mathbf{x}^1(t_0)$ of 0.002) using `ode45` in MATLAB. Fig. 24 shows a comparison of the optimized states to the propagated states of one of the spacecraft. It is apparent that the propagated states track fairly well to the optimized ones indicated that the 100 node solution is a good solution for preliminary design considerations.
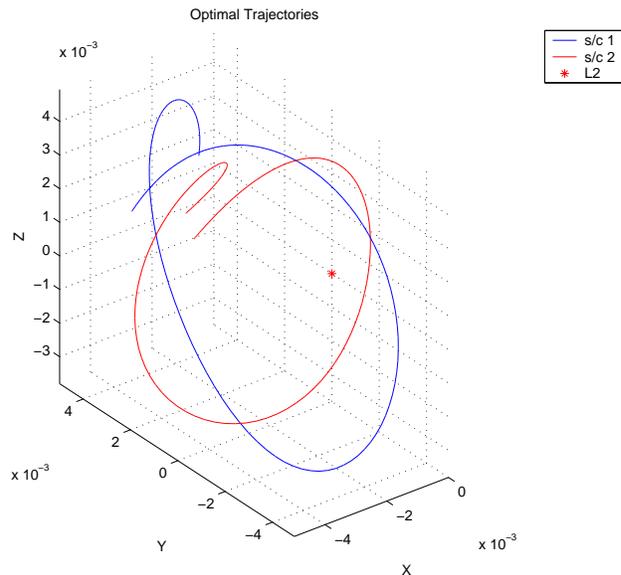

**Fig. 19   Trajectories for a large-baseline two-agent DSS**
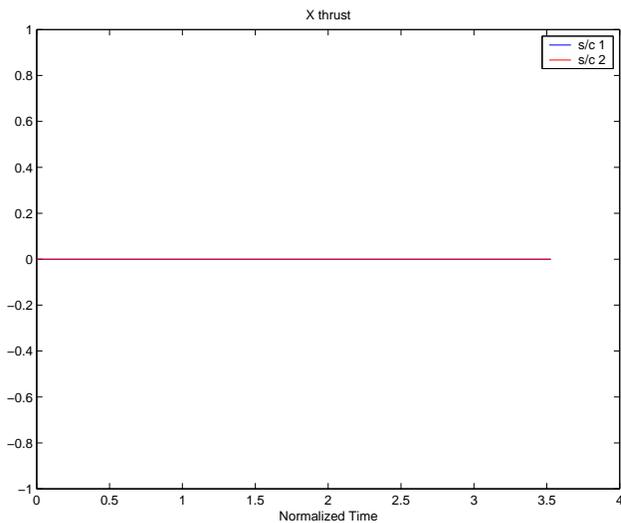
Fig. 20   Thrust along the x axis for the large-baseline two-agent DSS; note the scale on the ordinate
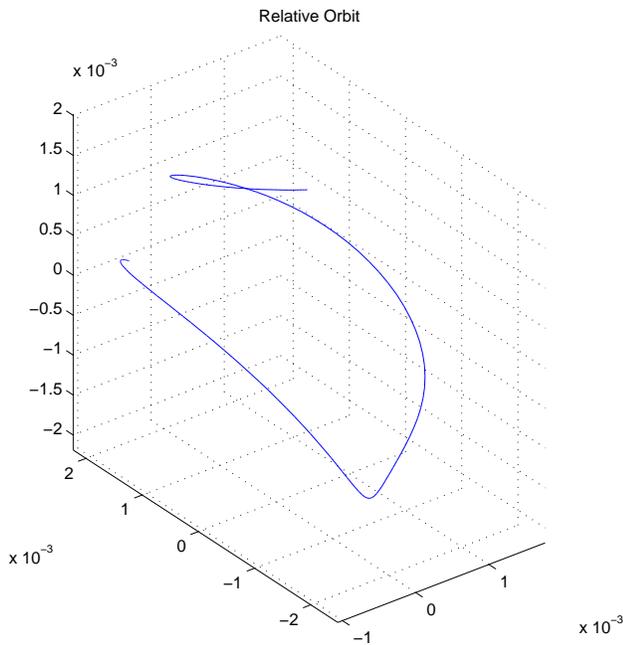
VI.   Conclusions

We presented a multi-agent-optimal-control framework for the design and control of spacecraft formations. This problem was discretized by the Legendre pseudospectral method and the resulting large-scale nonlinear programming problem was then solved by a sparse sequential quadratic programming method. These techniques are automated in the DIDO/SNOPT package which was used to solve the formation problem. Because there is no linearization in this framework, we can use the same technique and inputs for both small and large baseline formations, and find globally optimal (zero-cost) solutions for both with entirely different trajectories. We have shown that we can limit our results as needed to find specific types
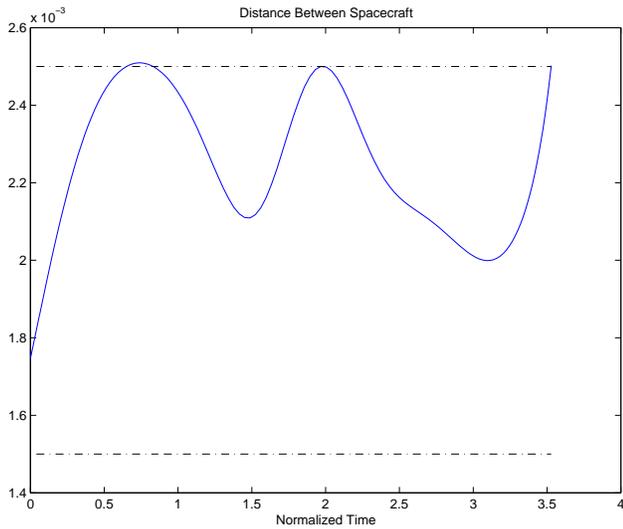
Fig. 21   Separation between the two spacecraft over time
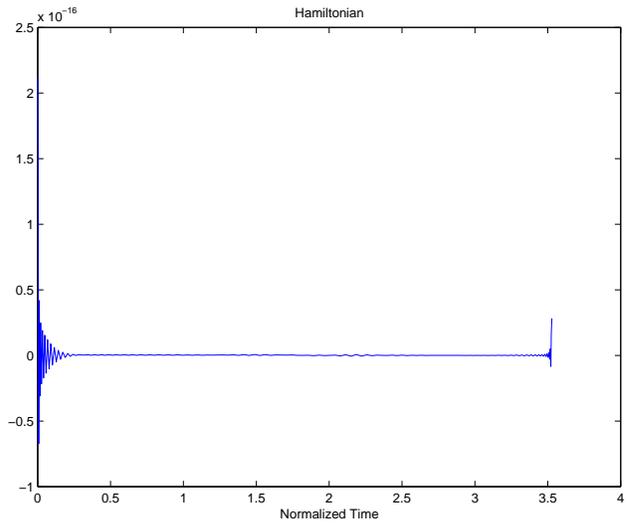
Fig. 23   Evolution of the Hamiltonian for the large-baseline two-agent DSS; note the scale on the ordinate

Fig. 22   Relative orbit for the large-baseline two-agent DSS

Fig. 24   Comparison of the position states of spacecraft one (solid) to those propagated by ODE45 in Matlab (dotted)

of formations by including different constraints (e.g. periodic conditions). This framework has this flexibility in applications with a simple consistent problem formation process because the design and control are approached concurrently.

References

[1]Tanner, H. G., Jadbabaie, A. and Pappas, G. J., "Stable Flocking of Mobile Agents, Part I: Fixed Topology," *Proceedings of the 42nd IEEE Conference on Decision and Control*, Maui, Hawaii, December 2003.

[2]*New World Vistas*, Summary Volume, USAF Scientific Advisory Board, December 1995.

[3]Vincent, M. A. and Bender, P. L., "The Orbital Mechanics of a Space-Borne Gravitational Wave Experiment," *Advances in*
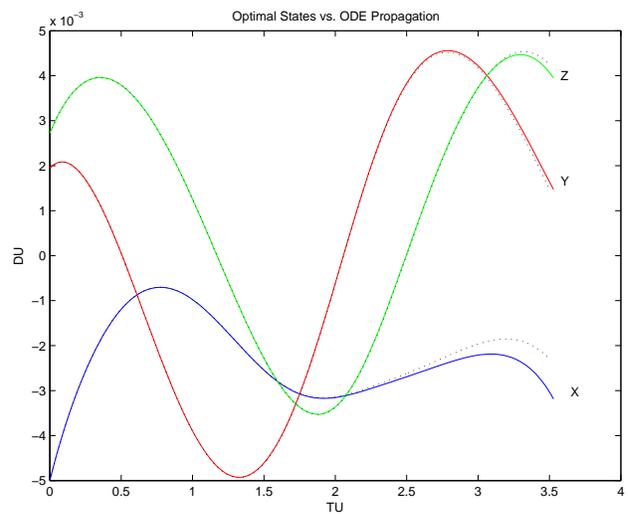
the Astronautical Sciences, Astrodynamics*, 1987, Vol. 65, Part II, Pg. 1346. Edited by Soldner, J.K. et al. Paper AAS 87-523. Full paper in AAS Microfiche Series, Vol.55.

[4]Ross, I. M., "A Mechanism for Precision Orbit Control With Applications to Formation Keeping," *Journal of Guidance, Control and Dynamics*, Vol.25, No. 4, 2002, pp. 818-820.

[5]Carpenter, R. J., Leitner, J. A., Folta, D. C. and Burns, R. D., "Benchmark Problems for Spacecraft Formation Flying Missions," *Proceedings of the AIAA Guidance, Navigation and Control Conference*, Austin, TX, August 2003, AIAA 2003-5364.

[6]Ross, I. M., King, J. T. and Fahroo, F., "Designing Optimal Spacecraft Formations," *Proceedings of the AIAA/AAS Astrodynamics Conference*, AIAA-2002-4635, Monterey, CA, 5-8 August 2002.

[7]King, J. T., "A Framework for Designing Optimal Spacecraft Formations," M. S. Thesis, Department of Aeronautical and Astronautical Engineering, Naval Postgraduate School, Monterey, CA, September 2002.

[8]Lindensmith, C. A., editor, "Technology Plan for the Terrestrial Planet Finder ", *JPL Publication 03-007*, 2003

[9]Fridlund, C.V.M., "Darwin - The Infrared Space Interferometry Mission," *ESA Bulletin*, 01 Aug 2000, Vol. 103, pp. 20-25

[10]Constellation X homepage http://constellation.gsfc.nasa.gov/

[11]National Security Space Road Map http://www.wslfweb.org/docs/roadmap/spacroad.htm

[12]Infeld, S. I. and Murray, W., "Optimization of Stationkeeping for a Libration Point Mission," *AAS Spaceflight Mechanics Meeting*, Maui, HI, February 2004. AAS 04-150.

[13]Marchand, B. G. and Howell, K. C., "Formation Flight Near L_1 and L_2 in the Sun-Earth/Moon Epheremis System Including Solar Radiation Pressure," AAS 03-596.

[14]Hsiao, F. Y. and Scheeres, D. J., "Design of Spacecraft Formation Orbits Relative to a Stabilized Trajectory," AAS 03-175.

[15]Hamilton, N. H., Folta, D. and Carpenter, R., "Formation Flying Satellite Control Around the L2 Sun-Earth Libration Point," *AIAA/AAS Astrodynamics Specialist Conference*, Monterey, CA, August 2002, AIAA 2002-4528.

[16]Gurfil, P. and Kasdin, N. J., "Dynamics and Control of Relative Motion in an Unstable Orbit," *AIAA/AAS Astrodynamics Conference*, Denver, CO, August 2000, AIAA 2000-4135.

[17]Gomez, G. Masdeont, J. and Simo, C., "Quasihalo Orbits Associated with Libration Points," *Journal of the Astronautical Sciences*, Vol.46, 1998, pp.135-176.

[18]Kim, M. and Hall, C. D., "Lyapunov and Halo Orbits about L_2," AAS 01-324.

[19]Richardson, D. L., "Analytic Construction of Periodic Orbits About the Collinear Points," *Celestial Mechanics*, Vol. 22, 1980, pp. 241253.

[20]Junge, O., Levenhagen, J. Seifried, A. and Dellnitz, M., "Identification of Halo Orbits for Energy Efficient Formation Flying," *Proceedings of the International Symposium on Formation Flying*, Toulouse, France, 2002.

[21]Serban, R., Koon, W. S., Lo, M. Marsden, J. E., Petzold, L. R., Ross, S. D. and Wilson, R. S., "Halo Orbit Mission Correction Maneuvers Using Optimal Control," *Automatica*, **38**, 2002, pp.571-583.

[22]Elnagar, J., Kazemi, M. A. and Razzaghi, M., "The Pseudospectral Legendre Method for Discretizing Optimal Control Problems," *IEEE Transactions on Automatic Control,* Vol. 40, No. 10, 1995, pp. 1793-1796.

[23]Ross, I. M., and Fahroo, F., "Legendre Pseudospectral Approximations of Optimal Control Problems," *Lecture Notes in Control and Information Sciences*, Vol.295, Springer-Verlag, New York, 2003.

[24]Ross, I. M. and Fahroo, F., "Pseudospectral Knotting Methods for Solving Optimal Control Problems," *Journal of Guidance, Control and Dynamics*, Vol.27, No.3, pp.397-405, 2004.

[25]Canuto, C., Hussaini, M. Y., Quarteroni, A., and Zang, T.A., *Spectral Methods in Fluid Dynamics,* Springer Verlag, New York, 1988.

[26]Betts, J. T., *Practical Methods for Optimal Control Using Nonlinear Programming,* SIAM: Advances in Control and Design Series, Philadelphia, PA, 2001.

[27]Gill, P. E., Murray, W., and Saunders, M. A., "SNOPT: An SQP Algorithm for Large-Scale Constrained Optimization," *SIAM Journal of Optimization*, Vol.12, No. 4, pp. 979-1006, 2002.

[28]Boggs, P. T. and Tolle, J. W., "Sequential Quadratic Programming," *Acta Numerica*, 1995, Cambridge University Press, Cambridge, UK, 1995, pp. 151.

[29]Ross, I. M., and Fahroo, F., "A Perspective on Methods for Trajectory Optimization," *Proceedings of the AIAA/AAS Astrodynamics Conference*, Monterey, CA, August 2002. AIAA Paper No. 2002-4727.

[30]Ross, I. M., "How to Find Minimum-Fuel Controllers," *Proceedings of the AIAA Guidance, Navigation and Control Conference*, Providence, RI, August 2004. AIAA Paper No. 2004-5346.

[31]F. H. Clarke, Y. S. Ladyaev, R. J. Stern and P. R. Wolenski, *Nonsmooth Analysis and Control Theory,* Springer-Verlag, New York, NY, 1998.

[32]Lo, M., B. G. Williams, W. E. Bollman, D. Han, Y. Hahn, J. L. Bell, E. A. Hirst, R. A. Corwin, P. E. Hong, K. C. Howell, B. Barden, and R. Wilson, "Genesis Mission Design," Paper No. AIAA 98-4468.

[33]Fischer, A., "Structure of Fourier Exponents of Almost Periodic Functions and Periodicity of Almost Periodic Functions," *Mathematical Bohemica*, No. 3, 1996, pp. 249-262.

[34]Corduneanu, C., *Almost Periodic Functions*, John Wiley, New York, 1968.

[35]Ross, I. M., Yan, H. and Fahroo, F., "A Curiously Outlandish Problem in Orbital Mechanics," *AAS/AIAA Astrodynamics Specialist Conference*, Quebec City, Canada, July 2001, AAS-01-430.

[36]Rockafellar, R. T., "Lagrange Multipliers and Optimality," *SIAM Review*, Vol.35, pp.183-283, 1993.

[37]Dontchev, A. L., Hager, W. W., and Veliov, V. M., "Second-Order Runge-Kutta Approximations in Control Constrained Optimal Control Problems," *SIAM Journal of Numerical Analysis*, Vo. 38, No. 1, 2000, pp. 202-226.

[38]J. T. Betts, N. Biehn and S. L. Campbell, "Convergence of Nonconvergent IRK Discretizations of Optimal Control Problems with State Inequality Constraints," *SIAM Journal of Scientific Computing* Vol. 23, No. 6, pp. 1981-2007, 2002.

[39]Bryson, A. E. and Ho, Y.-C., *Applied Optimal Control*, Hemisphere Publishing Corporation, Chapter 7, 1975.

[40]Hager, W. W., "Runge-Kutta Methods in Optimal Control and the Transformed Adjoint System," *Numerische Mathematik,* Vol. 87, 2000, pp. 247-282.

[41]Trefethen, L. N., *Spectral Methods in MATLAB,* SIAM, Philadelphia, PA, 2000.

[42]R. A. Adams, *Sobolev Spaces*, Academic Press, New York, N. Y., 1975.

[43]Gong, Q., Ross, I. M., Kang, W., and Fahroo, F., "Convergence of Pseudospectral Methods for Constrained Nonlinear Optimal Control Problems," *Intelligent Systems and Control*, Series on Modelling, Identification and Control, Acta Press, Calgary, Canada, 2004.

[44]Ross, I. M. and Fahroo, F., "User's Manual for DIDO 2002: A MATLAB Application Package for Dynamic Optimization," *NPS Technical Report, AA-02-002*, Department of Aeronautics and Astronautics, Naval Postgraduate School, Monterey, CA, June 2002.

[45]Holmström, K., Göran, A. O. and Edvall, M. M., "User's Guide for Tomlab 4.0.6," Tomlab Optimization, Sweden, August 2003.

[46]Ross, I. M. and Fahroo, F., "A Unified Computational Framework for Real-Time Optimal Control," *Proc.IEEE Conf. on Decision and Control,* Maui, HI, December 2003.

[47]Ross, I. M. and Fahroo, F., "Pseudospectral methods for optimal motion planning of differentially flat systems," *Proc.IEEE Conf. on Decision and Control,* Las Vegas, NV, December 2002; also, to appear in *IEEE Transactions of Automatic Control.*

[48]Strizzi, J. Ross, I. M and Fahroo, F., "Towards realtime computation of optimal controls for nonlinear systems," *Proceedings of the AIAA Guidance, Navigation, and Control Conference,* Monterey, CA, August 2002, AIAA Paper No. 2002-4945.

[49]Ross, I. M. and D'Souza, C. N., "Rapid Trajectory Optimization of Multi-Agent Hybrid Systems," *Proceedings of the AIAA GNC Conference*, Providence,RI, 2004. AIAA Paper No. 2004-5422.

⁵⁰Ross, I. M. and Fahroo, F., "Discrete Verification of Necessary Conditions for Switched Nonlinear Optimal Control Systems," *Proceedings of the American Control Conference*, June 2004, Boston, MA.

⁵¹Labeyrie, A., Le Coroller, H., Dejonghe, J. , Martinache, F., Borkowski, V., Lardire, O., Koechlin, L., "Hypertelescope imaging: from exo-planets to neutron stars," *Proceedings of SPIE conference*, vol. 4852, Hawaii, 2002.